Unexpected magnetism in low dimensional systems: the role of symmetry

2006 J. Phys.: Conf. Ser. 30 215

(http://iopscience.iop.org/1742-6596/30/1/026)

Institute of Physics Publishing Journal of Physics: Conference Series **30** (2006) 215–223
doi:10.1088/1742-6596/30/1/026 Symmetry and Structural Properties of Condensed Matter (SSPCM 2005)

Unexpected magnetism in low dimensional systems: the role of symmetry

MC Muñoz[1], L Chico[2], MP López-Sancho[1], JI Beltrán[1], S Gallego[1] and J Cerdá[1]

[1] Instituto de Ciencia de Materiales de Madrid, Consejo Superior de Investigaciones Científicas, Cantoblanco, 28049 Madrid, Spain
[2] Departamento de Física Aplicada, Facultad de Ciencias del Medio Ambiente, Universidad de Castilla-La Mancha, 45071 Toledo, Spain

E-mail: mcarmen@icmm.csic.es

Abstract.

The symmetry underlying the geometric structure of materials determines most of their physical properties. In low dimensional systems the role of symmetry is enhanced and can give rise to new phenomena. Here, we report on unexpected magnetism in carbon nanotubes and O-rich surfaces of ionic oxides, to show how its existence is closely related to the symmetry conditions. First, based on tight-binding models, we demonstrate that chiral carbon nanotubes present spin splitting at the Fermi level in the absence of a magnetic field, whereas achiral tubes preserve spin degeneracy. These remarkably different behaviors of chiral and non-chiral nanotubes are due to the intrinsic symmetry dependence of the spin-orbit interaction. Second, the occurence of spin-polarization at ZrO_2, Al_2O_3 and MgO surfaces is proved by means of *ab-initio* calculations within the density functional theory. Large spin moments develop at O-ended polar terminations, transforming the non-magnetic insulator into a half-metal. The magnetic moments mainly reside in the surface oxygen atoms, and their origin is related to the existence of $2p$ holes of well-defined spin polarization at the valence band of the ionic oxide. The direct relation between magnetization and local loss of donor charge shows that at the origin of these phenomena is the reduced surface symmetry.

1. Introduction

The underlying symmetry of a material is probably its most fundamental characteristic, since it determines not only the structure but also the macroscopic properties. Pure geometrical arguments are usually sufficient to understand qualitatively many physical properties of matter. When dimensions are reduced, the role of geometry and symmetry is enhanced and can give rise to new and unexpected phenomena. Together with its inherent fundamental interest, this has important technological consequences, auguring the birth of new technologies [1, 2].

Carbon-based materials are a unique example of how different spatial distributions of atoms result in materials with different properties. Carbon is the only element of the Periodic Table which presents stable structures of any dimensionality, from the three dimensional (3D) diamond to the zero-dimensional (0D) fullerenes. Even though the only difference between carbon-based materials is the relative position of the C atoms, their physical properties are dissimilar. To put an example, diamond -the hardest material in nature- is an insulator, while two-dimensional (2D) graphite is a semimetal. Carbon nanotubes (CNTs) are formed by rolling up a graphene sheet

into a cylinder, so the structure is one-dimensional (1D). Some tubes have a spiral conformation of atoms in the unit cell, they are called chiral tubes. They constitute a new class of mesoscopic 1D quantum systems [3] in which physical properties are intimately related to geometry. They can either be metals or semiconductors depending on their diameter and chirality [4, 5].

Ceramic oxides as ZrO_2, Al_2O_3 and MgO are non-magnetic ionic insulators. Their electronic structure can be roughly described as a valence band formed by the filled O $2p$ orbitals and a conduction band formed by the empty metal levels. The crystal can be described as a set of charged ions bonded by strong electrostatic forces, due to the large charge transfer from the metal cation to O. The resulting electronic charge distribution is highly localized in the neighborhood of the ion cores, with the transferred electrons closely bound to oxygen. Surfaces of ionic compounds can be polar or non-polar. In polar surfaces each atomic plane is formed solely by either oxygen anions or metals cations, resulting in an alternated distribution of negative and positive charged layers. Contrary, in the non-polar surfaces, atomic layers are neutral due to the presence of both anions and cations at the same plane. Formation of polar surfaces requires the modification of the charge density via faceting, reconstruction, changes of the surface stoichiometry or any alternative mechanism which disrupts their polar divergent character.

In this paper, we explore the close connection between magnetism and symmetry in low dimensional systems. We demonstrate that chiral carbon nanotubes and O-rich polar surfaces of binary insulating oxides present a magnetic ground state whose origin lies in the reduced symmetry of the structures [6, 7].

2. Model and method

2.1. Metallic carbon nanotubes

We model CNTs by a Slater-Koster [8] empirical tight-binding (ETB) hamiltonian including sp^3 orbitals, employing the Tománek-Louie parametrization for graphite [9] to take into account the actual discrete nature of the lattice, and including the spin-orbit interaction (SOI). The unit cell is generated by rolling up a portion of graphene layer, thus including curvature effects [10]. Metallic tubes present a band crossing at the Fermi level either at Γ or at two thirds of the distance from Γ to the zone boundary [6]; here we focus on 2/3-metals CNTs.

SOI is caused by the coupling of the spin of a moving electron with an electric field which acts as a magnetic field in the rest frame of the electron. In a crystalline environment, the major internal contribution arises from the electron orbital motion in the crystal potential V, and thus its effects are related to the crystal symmetry. The SOI is given by $H_{SO} = \frac{\hbar}{4mc^2}\sigma(\nabla V \times \mathbf{p})$, where σ represents the Pauli matrices and $\mathbf{p}$ the electron momentum. The relevant contribution of the crystal potential is that close to the atomic cores, so assuming spherical symmetry, the above hamiltonian can be expressed as $H_{SO} = \lambda \mathbf{L} \cdot \mathbf{S}$, where the spin-orbit (SO) coupling constant (λ) depends on the atomic orbital and $\mathbf{L}$ is the angular momentum of the electron. Within the ETB framework, H_{SO} couples p orbitals on the same atom, and λ can be either greater or smaller than the atomic value [11, 12]. The present calculations have been performed with $\lambda = 0.2$ eV [6]. SO effects have been customarily neglected in graphite-like materials, and the exact value of λ is not known. Although there are no recent measurements, low dimensionality, electron-electron interactions and magnetic fields are shown to induce an enhancement of SO coupling [13, 14, 15]. Nevertheless, the SO strength can be controlled by a proper choice of gate potentials [16], as was first proposed for semiconductor heterostructures.

2.2. Surfaces of ionic oxides

We have studied low-index surfaces of binary insulating oxides of different crystal structures: MgO, Al_2O_3 and ZrO_2. MgO adopts the rock-salt lattice. α-Al_2O_3 can be viewed as an hexagonal close-packed array of O atoms with the Al atoms occupying two thirds of the interstitial octahedral sites. ZrO_2 displays three polymorphs at room temperature [18], either in

its pure form (m-ZrO_2, monoclinic), or by dopage with substitutional cations (t-ZrO_2, tetragonal, and c-ZrO_2, cubic). The cubic structure corresponds to the CaF_2 lattice. t-ZrO_2 can be obtained from the cubic unit cell elongating one of the equivalent edges of the cube and introducing small opposite shifts at the O sublattice positions. The m-ZrO_2 lattice is more complex and has lower symmetry; it is formed by further distorting the tetragonal structure, with non-orthogonal lattice vectors. Depending on the crystallographic orientation, the stacking of atomic planes of the above lattices leads to very different surface structures. Perhaps the best example is c-ZrO_2(111), which shows three polar terminations labelled according to the composition of the two topmost layers: O-O-, O-Zr- and Zr-O-. Here we have considered all low-index terminations of c-ZrO_2, and selected t-ZrO_2, m-ZrO_2, MgO and Al_2O_3 surfaces: MgO(111) consists of a stacking of alternated pure Mg and O planes; in α-Al_2O_3(0001) consecutive O planes are separated by two Al layers; m-ZrO_2(001) defines a layered structure of chemical stacking sequence O-O-Zr, while c-ZrO_2(001) shows an alternance of O and Zr planes.

Our results are obtained from first-principles spin-polarized calculations within the DFT (density functional theory) under the GGA (generalized gradient approximation) for exchange and correlation [19]. We use the SIESTA package [24, 25] with basis sets formed by double-zeta polarized localized numerical atomic orbitals. More details about the conditions of the calculations can be found elsewhere [7, 26]. Each surface is modelled as a periodic slab containing a vacuum region of 10 Å. The width of the vacuum region is enough to inhibit interaction between neighbouring surfaces. The number of M_xO_y units in a slab -M being the metal donor and x,y accounting for the particular metal to oxygen ratio- depends on the particular structure, and ranges from 5 to 7. The slabs are symmetric about the central plane, to avoid an artificial divergent Madelung energy, although we have verified that all the conclusions of this work remain unaltered if asymmetric slabs are considered instead. Bulk-like behaviour is attained at the innermost central layers. The atomic positions are allowed to relax until the forces on the atoms are less than 0.06 eV/Å. For comparison, a non-spin polarized (NSP) calculation is also performed for each case.

3. Results and Discussion

3.1. Metallic carbon nanotubes

From symmetry considerations, the bands of any nanotube are at most fourfold degenerate. Considering spin, the bands crossing at E_F in 2/3-metals are only doubly degenerate. Thus, neglecting curvature effects, there is an accidental fourfold degeneracy at E_F in all 2/3-metals CNTs. First, we focus on achiral armchair tubes which possess inversion symmetry. Figure 1a presents the atomic structure and the spin-resolved density of states (DOS) of an armchair (5,5) CNT calculated at $\mathbf{k_F}$ for energies around the Fermi level, with and without SO coupling. It clearly shows that, even though armchair tubes remain metallic after including curvature effects (DOS calculated without SOI), the inclusion of SO interaction leads to a small gap opening as predicted by Ando [27]. The experimental measurement of the SO-induced gap could provide a way to estimate the SO-interaction strength. However, the spin degeneracy is not lifted by the SO interaction, although the states are no longer spin eigenstates. The eigenfunctions (not shown here) do not correspond to pure spin-states, although they have a dominant weight of one spin orientation. Thus, as was previously pointed out [27], due to the SOI in achiral CNTs, spin scattering is induced even by spin-independent scatterers and impurities can cause spin-relaxation.

Figure 1b shows the atomic structure and the corresponding DOS of a chiral (7,1) tube. Chiral NTs do not have an inversion center and only possess spiral symmetry operations. In contrast to the results shown for the (5,5) armchair CNT, curvature effects open a small gap at the Fermi energy (see DOS calculated without SOI). Further, the SO interaction lifts all degeneracies producing an energy splitting between states with different spin orientation in

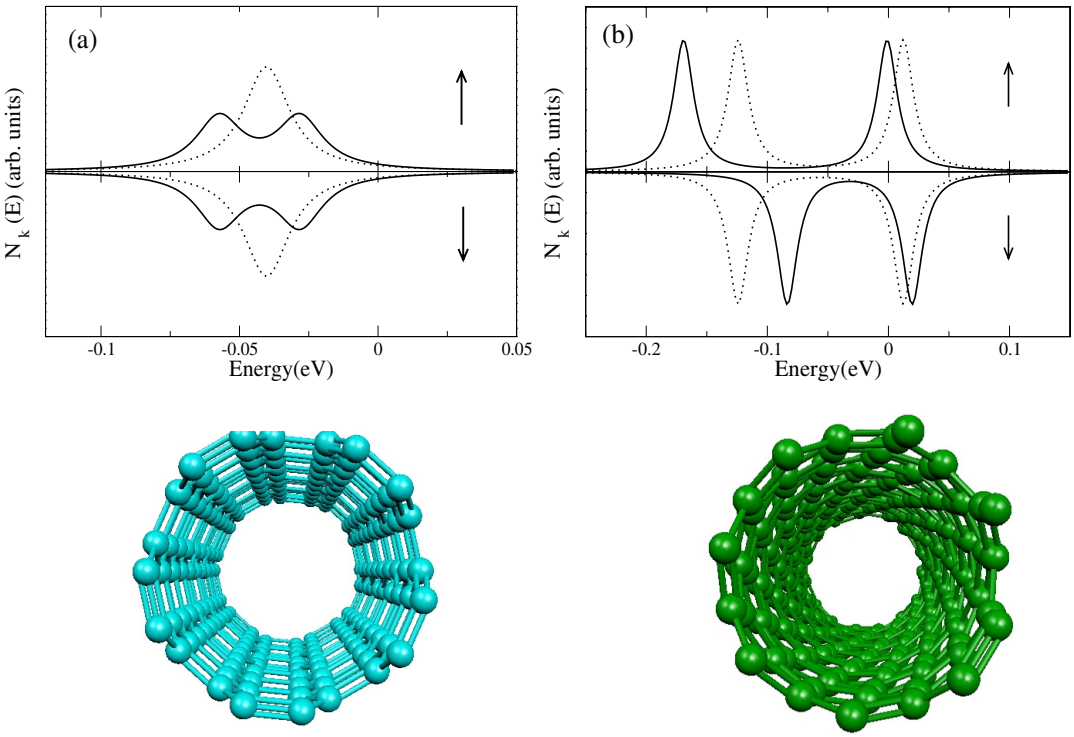

Figure 1. Atomic structure and spin-resolved DOS at $\mathbf{k_F}$ for (a) the (5,5) nanotube and (b) the (7,1) nanotube, calculated with (full line) and without (dotted line) SO interaction.

chiral nanotubes. The bands correspond to spin eigenstates. The motion of electrons with spin up and spin down are completely decoupled. Thus, in chiral CNTs there is not spin scattering from scatterers with a spin-independent potential. In fact, an electron with spin up cannot be scattered into a state with spin down and viceversa. This would explain the huge spin-flip scattering length ($\approx$ 130 nm) observed for spin-polarized electrons injected into multiwall CNTs [28]. In all tubules the band-crossing at E_F is between energy bands of different symmetry; then they respond differently to the SOI interaction, as can be seen in the figure since the SO splitting is band dependent.

SO-related effects in CNTs have a fundamental symmetry dependence: while in achiral tubes they do not affect the spin degenerate states, in chiral tubes spin degeneracy is completely removed. The origin of the asymmetric behavior of achiral and chiral CNTs under the SOI is due to the interplay of time reversal and spatial inversion symmetries. Kramers' theorem on time reversal symmetry states that $E_{\mathbf{k},\sigma} = E_{-\mathbf{k},-\sigma}$, where $E_{\mathbf{k},\sigma}$ is the energy of the eigenstate with wavevector $\mathbf{k}$ and spin σ. In achiral tubes, because there is an inversion center: $E_{\mathbf{k},\sigma} = E_{-\mathbf{k},\sigma}$, therefore, $E_{\mathbf{k},\sigma} = E_{\mathbf{k},-\sigma}$ and spin degeneracy can not be removed. For chiral tubes only the condition imposed by the time reversal invariance holds and thus spin degeneracy is lifted. In that case, electron velocities become dependent on both the spin and the direction of the motion.

The different response to the SOI of chiral CNT bands of different symmetry can lead to sequences of states with parallel spin. Such effect occurs at energies around a band gap and whenever there are two bands close in energy with different symmetry. This is illustrated in Figure 2, which shows the spin-resolved DOS of a chiral (9,3) CNT for energies around the Fermi level. Recently, spin-dependent transport experiments have been reported which were in apparent contradiction, suggesting the existence of different spin ground states in CNTs. On one

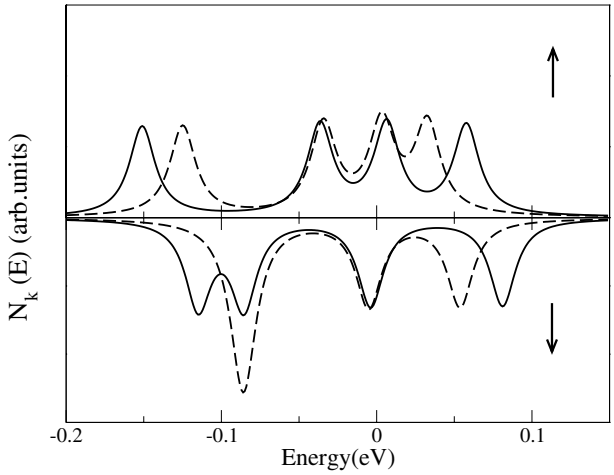

Figure 2. Spin-resolved DOS for the (9,3) tube at $\mathbf{k} = 0.025$ (full line), and $\mathbf{k} = 0.0125$ (dashed line). Wavevector values are given with respect to the BZ length.

hand, measurements performed at low magnetic fields in a bundle of CNTs [29] and in quantum dots [30, 31] found the expected spin alternation and could be explained by a simple shell-filling model. On the other, successive electrons entering isolated CNTs showed that consecutive electrons could have the same spin-direction, indicating a possible spin polarization of the nanotube [32]. This experimental observation could be explained by the sequential ordering of states with parallel spin [6]. We have focused in metallic tubes, but SO-induced spin splitting is also present in chiral semiconductor tubes, where SO-related effects are analogous.

3.2. Surfaces of ionic oxides

Table 1 summarizes our main result. It shows the total magnetic moments at the surface oxygen plane for all the structures which present a magnetic ground state, together with their in-plane ($||$) and normal ($\perp$) p projections onto the surface. All spin moments arise almost exclusively from the p electrons at the valence band of the oxide. They reach large values, ranging from 0.8 to 1.6 μ_B. Notice that only the O-rich oxide surfaces are magnetic. Both the cation-ended and the non-polar O surfaces not in the table do not show any spin polarization.

The distinct characteristic of all these magnetic structures is that they are polar divergent surfaces [33] with a loss of cationic coordination for the outermost O atoms. The loss of the surface O counterparts at the M_xO_y coordination unit leads to an asymmetric charge distribution and to the creation of *2p* holes at the oxide valence band. This already suggests that the O spin polarization is intimately related to the decrease of the oxygen ionic charge at the surface with respect to the bulk, that is, to the existence of *2p* holes at the valence band. The correlation is evident after inspection of Table 1, where the rightmost columns provide the oxygen Mulliken populations at the surface layer and the bulk. In all these cases the surface oxygen loses ionic charge approaching a charge neutral state. Moreover, the smaller the oxygen ionic charge, the larger its associated magnetic moment.

The calculated surfaces with a non-magnetic ground state have oxygen charges close to the bulk ones, which corroborates the correlation between the reduction of the ionic charge and the formation of the magnetic moment. As an example, we can compare the surface O Mulliken populations of the two O-ended c-ZrO_2(111) surfaces. O atoms at the O-O- surface -which presents a high magnetic moment of 1.6 μ_B- have an ionic charge of 6.02, while that corresponding to the non-magnetic O-Zr- surface is 6.68, closer to the 6.79 obtained for bulk oxygen. This means that the spin polarization is a response of the system to the loss of

Table 1. Spin moments (in μ_B) at the topmost layer of all the oxide surfaces with a magnetic ground state, together with the decomposition of the p orbital contribution parallel and normal to the surface plane. The rightmost columns provide the corresponding Mulliken charge populations (Q) compared to the inner bulk value (Q_b). The O_1 and O_2 entries for the non-cubic ZrO_2 structures refer to the two inequivalent in-plane positions.

Surface	$\mathbf{m}_{tot}$	$m^p{}_{\|\|}$	$m^p{}_{\perp}$	**Q**	Q_b
c-$ZrO_2(111)_{O-O-}$	**1.56**	1.50	0.04	**6.02**	6.79
m-ZrO_2(001)-O_1	**1.43**	0.81	0.61	**6.10**	6.66
-O_2	**1.43**	0.81	0.60	**6.11**	
t-ZrO_2(001)-O_1	**1.19**	0.54	0.64	**6.13**	6.76
-O_2	**0.59**	0.55	0.03	**6.17**	
c-ZrO_2(001)	**0.83**	0.62	0.21	**6.29**	6.79
Al_2O_3(0001)	**0.97**	0.74	0.23	**6.10**	6.49
MgO(111)	**0.83**	0.06	0.76	**6.37**	6.72

transferred charge.

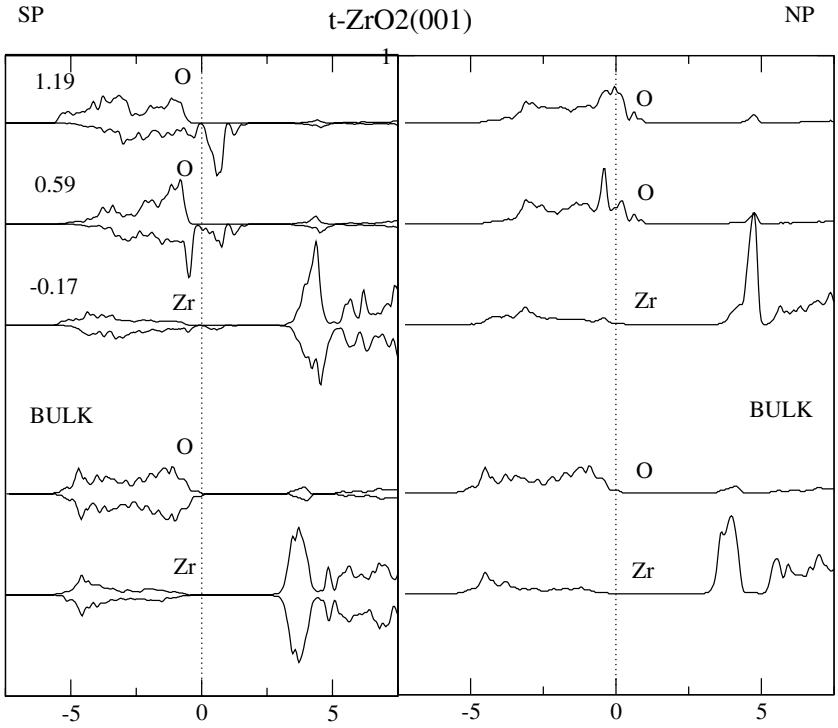

Figure 3. DOS for the three topmost planes and the bulk of t-ZrO_2(001) after SP (left) and NSP (right) calculations. Positive (negative) values correspond to majority (minority) spin states. Energies are referred to the Fermi level. The total spin moments at each layer are indicated for the SP case.

All the magnetic surfaces are half-metallic. Figure 3 shows the spin-resolved density of states (DOS) at the three uppermost layers and the bulk for the t-ZrO_2(001) surface, both for SP (left) and NSP (right) calculations. As in all the magnetic structures investigated, the Fermi level (E_F)

crosses the valence band of the topmost layer. Remarkably, the bands crossing E_F have always a well defined spin polarization, the majority spin states being full while the minority spin band is partially filled. The result is a half-metallic system. The most significant effect of the spin exchange is the shift of the minority spin DOS and the reduction of the DOS at E_F. However, a deep redistribution of charge occurs, as manifests the shape of the surface oxygen DOS; the changes of the electronic distribution affect mostly to the minority spin electrons. Even if the magnetization is a local effect, rooted in the lack of donor electrons for the outermost O atoms, the spin polarization at the surface layer induces a magnetic moment at the neighbouring planes, which decays as we deepen into the bulk. This can be observed in Figure 3, which provides the magnetization of the three surfacemost layers for t-ZrO_2(001). A similar trend corresponds to all magnetic surfaces calculated here.

The major changes observed in the DOS are also present in the spatial charge distributions. This can be directly seen in the left and central panels of Figure 4, which depict the spin-resolved charge density differences (CDD, total charge density minus the superposition of atomic charge densities) of the [0001] α-Al_2O_3 surface, within a plane normal to the surface along the bond direction between a surface O atom and a nearest neighbour at the consecutive O layer. The majority spin band being completely filled, as was shown in the DOS, the corresponding surface CDD adopts the spherical symmetry of the bulk. On the contrary, anisotropic lobular shapes appear in the minority spin charge. This asymmetry between the spatial distributions of the spin states is a common feature to all the magnetic structures studied here. The rightmost panels of the figure show the corresponding spin density difference (SDD), CDD of majority spin minus CDD of minority spin. The crystal field induces directionality to the spin moments, involving orbitals along specific directions. For the [0001] α-Al_2O_3 surface the dominant contribution comes from orbitals contained within the surface plane, although there is a significant contribution to the magnetic charge from orbitals normal to the surface.

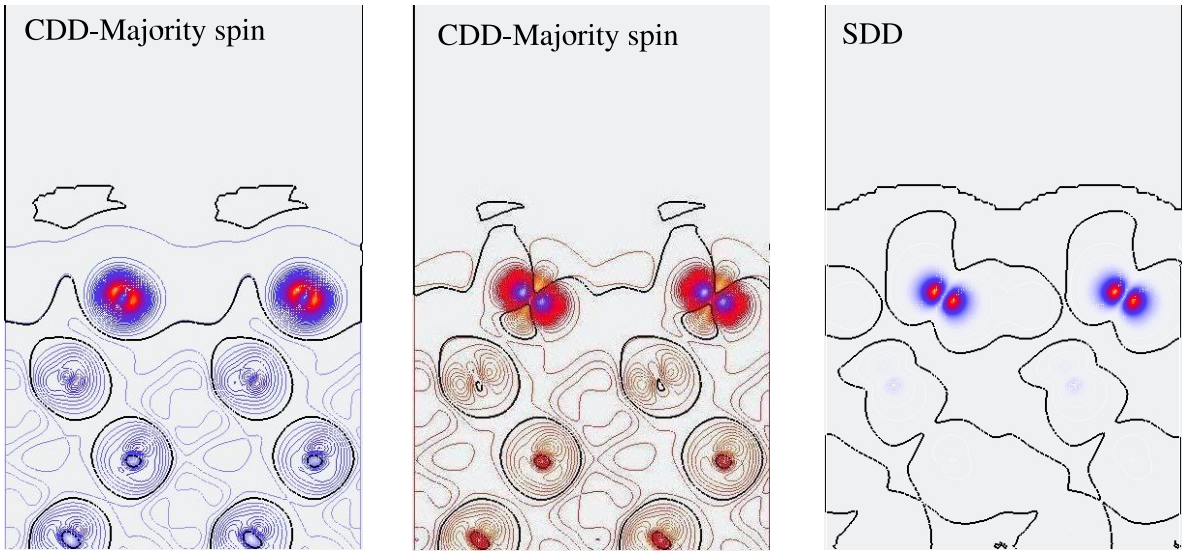

Figure 4. Left and middle panels: spin-resolved CDD for the α-Al_2O_3(0001) surface. Right panel: corresponding SDD.

Very recently, unexpected ferromagnetism has been measured in thin films of undoped non-magnetic oxides, like HfO_2 and ZrO_2, and assigned to the presence of lattice defects concentrated at the film interface. [34, 35]. The mechanism presented here provides an explanation for the origin of the magnetic moments of these so called d^0 ferromagnets. Furthermore, we predict

that this kind of magnetism can be extended to a wider class of non-magnetic oxides, like MgO and Al_2O_3, where the cation is not necessarily a d metal.

4. Conclusions

In summary, we have shown that low dimensional systems as carbon nanotubes and surfaces of ionic oxides present new and unexpected magnetism directly related to their reduced symmetry. The SO interaction removes spin degeneracy in chiral CNTs due to the lack of inversion symmetry of the crystal potential, while in achiral CNTs spin degeneracy is not lifted. Thus, SO interaction in CNTs presents an intrinsic symmetry dependence. In addition, we have proved the existence of local magnetism at the ideal O-ended polar surfaces of ceramic oxides. Large spin moments are formed at the outermost surface plane due to the lack of donor charge and the subsequent creation of $2p$ holes in the valence band of the oxide. This leads to a half-metallic ground state, with the majority spin band completely filled and only minority spin states at the Fermi level. The fact that low dimensional materials exhibit a 100 % spin polarization at the Fermi level opens a new route to the manipulation of spin currents.

Acknowledgments

This work has been partially financed by the Spanish Ministerio de Educación y Ciencia and the DGES under contracts MAT2002-04095-C02-01, MAT2002-04540-C05-03 and MAT2003-04278, and by the Comunidad Autónoma de Madrid under CAM2004-0440. S.G. acknowledges financial support from the Ramón y Cajal program of the Spanish Ministerio de Educación y Ciencia, and J.I.B. from the I3P program of the CSIC.

5. References

[1] Wolf S A *et al* 2001 *Science* **294** 1488
[2] Prinz G A 1998 *Science* **282** 1660
[3] Saito R, Dresselhaus G and Dresselhaus M 1998 *Physical Properties of Carbon Nanotubes*, London (Imperial College Press)
[4] Wildöer J W G *et al.* 1998 *Nature* **391** 59
[5] Odom T W *et al.* 1998 *Nature* **391** 62
[6] Chico L, López-Sancho M P and Muñoz M C 2004 *Phys. Rev. Lett.* **93** 176402
[7] Gallego S, Beltran J I, Cerdá J and Muñoz M C 2005 *J. Phys.: Condens. Matter* **17** L451
[8] Slater J C and Koster J F 1954 *Phys. Rev.* **94** 1498
[9] Tománek D and Louie S G 1988 *Phys. Rev. B* **37** 8327
[10] Blase X *et al.* 1994 *Phys. Rev. Lett.* **72** 1878
[11] Wang C S and Callaway J 1974 *Phys. Rev. B* **9** 4897
[12] Gallego S and Muñoz M C 1999 *Surf. Sci.* **423** 324
[13] Moroz A V and Barnes C H W 1999 *Phys. Rev. B* **60** 14272
[14] Chen G H and Raikh M E 1999 *Phys. Rev. B* **60** 4826
[15] Valín-Rodríguez M 2004 *Phys. Rev. B* **70** 033306
[16] Rashba E I and Efros A L 2003 *Phys. Rev. Lett.* **91** 126405
[17] Kleiner A and Eggert S 2001 *Phys. Rev. B* **63** 73408
[18] Howard C J, Hill R J and Reichert B E 1988 *Acta Crystallogr. Sect. B: Struct. Sci.* **44** 116
[19] Perdew J P *et al.* 1992 *Phys. Rev. B* **46** 6671
[20] Kralik B, Chang E K and Louie S G 1998 *Phys. Rev. B* **57** 7027
[21] Jansen H J F 1991 *Phys. Rev. B* **43** 7267
[22] Eichler A 2001 *Phys. Rev. B* **64** 174103
[23] Zhao X and Vanderblit D 2002 *Phys. Rev. B* **65** 075105
[24] Ordejón P, Artacho E and Soler J M 1996 *Phys. Rev. B* **53** R10441
[25] Soler J M *et al.* 2002 *J. Phys.: Condens. Matter* **14** 2745
[26] J.I. Beltrán *et al.*, *Phys. Rev. B* **68**, 075401 (2003).
[27] Ando T 2000 *J. Phys. Soc. Jpn.* **69** 1757
[28] Tsukagoshi K, Alphenaar B W and Ago H 1999 *Nature* **401** 572
[29] Cobden D H *et al.* 1998 *Phys. Rev. Lett.* **81** 681

[30] Cobden D H and Nygård J 2002 *Phys. Rev. Lett.* **89** 046803
[31] Liang W, Bockrath M and Park H 2002 *Phys. Rev. Lett.* **88** 126801
[32] Tans S J *et al.* 1998 *Nature* **394** 761
[33] Tasker P W 1979 *J. Phys. C: Sol. State Phys.* **12** 4977
[34] Venkatesan M, Fitzgerald C B and Coey J M D 2004 *Nature* **430** 630
[35] M. Coey, Abstract U5.00005 of 2005 APS March Meeting